JACS
JOURNAL OF THE AMERICAN CHEMICAL SOCIETY
Article
pubs.acs.org/JACS

# Visible-Light-Induced Water Splitting Based on Two-Step Photoexcitation between Dye-Sensitized Layered Niobate and Tungsten Oxide Photocatalysts in the Presence of a Triiodide/Iodide Shuttle Redox Mediator

Ryu Abe,*[,†,§,∥] Kenichi Shinmei,[†] Nagatoshi Koumura,[‡] Kohjiro Hara,[‡] and Bunsho Ohtani[†]

[†]Catalysis Research Center, Hokkaido University, Sapporo 001-0021, Japan
[‡]National Institute of Advanced Industrial Science and Technology (AIST), Tsukuba 305-8571, Japan
[§]JSPS-NEXT Program, Koujimachi, Chiyoda-ku, Tokyo 102-0083, Japan

**ABSTRACT:** Water splitting into $H_2$ and $O_2$ under visible light was achieved using simple organic dyes such as coumarin and carbazole as photosensitizers on an n-type semiconductor for $H_2$ evolution, a tungsten(VI) oxide ($WO_3$) photocatalyst for $O_2$ evolution, and a triiodide/iodide ($I_3^-/I^-$) redox couple as a shuttle electron mediator between them. The results on electrochemical measurements revealed that the oxidized states of the dye molecules having an oligothiophene moiety (two or more thiophene rings) in their structures are relatively stable even in water and possess sufficiently long lifetimes to exhibit reversible oxidation−reduction cycles, while the carbazole system required more thiophene rings than the coumarin one to be substantially stabilized. The long lifetimes of the oxidized states enabled these dye molecules to be regenerated to the original states by accepting an electron from the $I^-$ electron donor even in an aqueous solution, achieving sustained $H_2$ and $I_3^-$ production from an aqueous KI solution under visible light irradiation when they were combined with an appropriate n-type semiconductor, ion-exchangeable layered niobate $H_4Nb_6O_{17}$. The use of $H_4Nb_6O_{17}$ loaded with Pt cocatalyst inside the interlayer allowed the water reduction to proceed preferentially with a steady rate even in the presence of a considerable amount of $I_3^-$ in the solution, due to the inhibited access of $I_3^-$ to the reduction site, Pt particles inside, by the electrostatic repulsion between the $I_3^-$ anions and the negatively charged $(Nb_6O_{17})^{4-}$ layers. It was also revealed that the $WO_3$ particles coloaded with Pt and $IrO_2$ catalysts exhibited higher rates of $O_2$ evolution than the $WO_3$ particles loaded only with Pt in aqueous solutions containing a considerable amount of $I^-$, which competitively consumes the holes and lowers the rate of $O_2$ evolution on $WO_3$ photocatalysts. The enhanced $O_2$ evolution is certainly due to the improved selectivity of holes toward water oxidation on $IrO_2$ cocatalyst, instead of undesirable oxidation of $I^-$. Simultaneous evolution of $H_2$ and $O_2$ under visible light was then achieved by combining the $Pt/H_4Nb_6O_{17}$ semiconductor sensitized with the dye molecules having an oligothiophene moiety, which can stably generate $H_2$ and $I_3^-$ from an aqueous KI solution, with the $IrO_2$−Pt-loaded $WO_3$ photocatalyst that can reduce the $I_3^-$ back to $I^-$ and oxidize water to $O_2$.

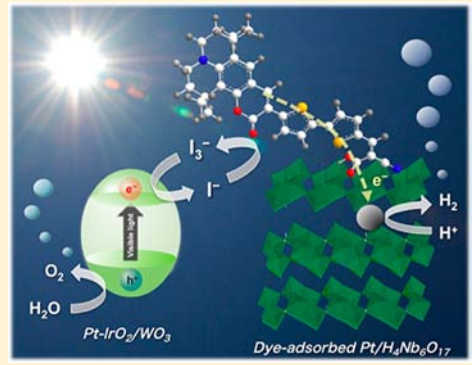


## 1. INTRODUCTION

Photoinduced water splitting into $H_2$ and $O_2$ using semiconductor materials has recently been a cutting-edge research area due to the growing expectation for clean and direct production of $H_2$ from water by utilizing abundant solar light.[1−9] Although a large number of metal oxide semiconductors have so far been demonstrated to be active photocatalysts for simultaneous evolution of $H_2$ and $O_2$ with the stoichiometric ratio 2:1, almost all of the active photocatalysts can utilize only ultraviolet (UV) light with a wavelength shorter than 400 nm, with quite rare exceptions, because of their larger bandgap energies than 3.0 eV. Since visible light accounts for nearly 50% of solar light energy that reaches the Earth's surface, efficient utilization of visible light is undoubtedly necessary to realize practically efficient $H_2$ production on a huge scale. The development of efficient water-splitting systems that can harvest a wide range of visible light has therefore been a great challenge over many years.[10−29] Applying a two-step photoexcitation system, a so-called Z-scheme, consisting of two different photocatalysts and a shuttle redox couple (Red/Ox)[30] is one of the promising strategies for achieving efficient water-splitting under visible light irradiation.[10−14,18−29] In this concept, the water-splitting system is separated into two components: one for $H_2$ evolution and the other for $O_2$ evolution. The photoexcited electrons on the $H_2$-evolving photocatalyst reduce water to $H_2$, and the holes generated oxidize a reductant (Red) to an oxidant (Ox). The Ox produced is then reduced back to the Red by the photoexcited electrons on the $O_2$-evolving photocatalyst

**Received:** May 15, 2013
**Published:** October 15, 2013

   dx.doi.org/10.1021/ja4048637 | J. Am. Chem. Soc. 2013, 135, 16872−16884

where the holes simultaneously oxidize water to $O_2$. On the basis of this concept, we demonstrated the first example of visible-light-induced water splitting in 2001 by using $SrTiO_3$ codoped with Cr and Ta as a $H_2$-evolving photocatalyst, $WO_3$ as an $O_2$-evolving photocatalyst, and an iodate/iodide ($IO_3^-$/$I^-$) redox couple[31] as a shuttle electron mediator.[10,11,13] Various combinations of $H_2$- and $O_2$-evolving photocatalysts have already afforded simultaneous evolution of $H_2$ and $O_2$ under visible light irradiation through the redox cycle of $IO_3^-$/$I^-$.[10,11,13,14,19,20,22,25−28] Introduction of the two-step photoexcitation concept (Z-scheme) can lower the energy required to drive each photocatalysis process, enabling one to utilize visible light more easily than in conventional one-step water-splitting systems consisting of a single photocatalyst. For example, the Z-scheme water-splitting system employing a mixed tantalum oxynitride $BaTaO_2N$ as the $H_2$-evolving photocatalyst was demonstrated to be photoactive at wavelengths up to ca. 660 nm,[20,22,28] the longest among the photocatalytic water-splitting systems so far reported. Kudo and his co-workers have also reported water splitting under visible light based on the Z-scheme with shuttle redox couples such as $Fe^{3+}/Fe^{2+}$ and $[Co(bpy)_3]^{3+}/[Co(bpy)_3]^{2+}$,[12,18,21,29] or even without any redox mediator.[23]

However, only a limited number of semiconductor materials are available for the visible-light-driven water splitting systems at present. The limitation basically arises from the difficulty in tailoring the band levels, as well as the bandgaps, of inorganic semiconductor materials. Scaife pointed out in 1980 the difficulty in developing an oxide semiconductor having both a sufficiently negative conduction band bottom for $H_2$ evolution and a narrow bandgap for visible light absorption.[32] Since the valence bands of oxide semiconductors are dominantly formed by O 2p orbitals, the top of the valence band is fixed at highly positive levels at around +3.0 V vs SHE, with rare exceptions.[32] Consequently, the conduction band bottoms of visible-light-responsive oxide semiconductors, which have narrower bandgaps than 3.0 eV, are generally insufficient for the water reduction (0 V vs SHE). In contrast, the fine-tuning of energy levels (HOMO and LUMO), as well as the energy gaps, of organic semiconductors is much easier than those of inorganic semiconductors.[33] It has been demonstrated that a number of organic dyes,[34−42] as well as metal complexes,[43] have both the sufficiently negative LUMO level for the electron injection to the conduction band of $TiO_2$ and the sufficiently positive HOMO level for the oxidation of $I^-$ to $I_3^-$ in organic solvents such as acetonitrile, and thus can be used as efficient photosensitizers in dye-sensitized solar cells.[34−43] It therefore appears that employing a dye-sensitized n-type semiconductor (e.g., $TiO_2$) as a $H_2$-evolving photocatalyst with $I^-$ electron donor is one of the reasonable approaches for establishing the Z-scheme water splitting systems that can harvest a wide range of visible light.

Figure 1 depicts $H_2$ evolution processes over a dye-sensitized n-type semiconductor. Upon irradiation of visible light, an electron is excited from the HOMO to LUMO of the dye molecule, and then injected into the conduction band of the semiconductor, generating an oxidized state of the dye molecule. The injected electrons transfer to a reduction site, such as Pt particles, and then reduce water to $H_2$. The oxidized state of the dye molecule can be regenerated to the original state by accepting an electron from an appropriate electron donor (Red) such as $I^-$, simultaneously generating an oxidized product (Ox) such as $I_3^-$. Although a considerable number of

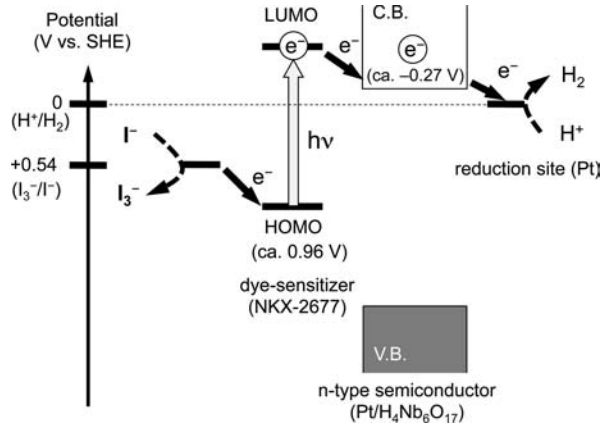


**Figure 1.** Conceptual scheme of $H_2$ evolution from water over a dye-sensitized n-type semiconductor using iodide ($I^-$) as an electron donor, with the energy diagram for the coumarin NKX-2677 dye system.

studies have been made on the dye-sensitized $H_2$ production using a strong sacrificial electron donor such as triethanolamine,[44] only a few reliable studies have so far been reported on nonsacrificial $H_2$ production employing a reversible electron donor such as $I^-$.[45−49] Both the insufficient stability of the oxidized state of simple dye molecules in aqueous media and the low efficiency in the regeneration process, the electron injection from the electron donor to the oxidized state,[48,49] seem to be the main reasons for the difficulty in achieving steady $H_2$ evolution from water using reversible electron donors such as $I^-$.

Among various organic dyes examined, a coumarin dye (C-343) adsorbed on a Pt-loaded $TiO_2$ particle was found to be active for $H_2$ evolution from an aqueous solution containing $I^-$ electron donor,[48,49] while the activity gradually decreased with prolonged irradiation time due to the gradual degradation of dye molecules. We have then revealed that inserting an oligothiophene (two or more thiophene rings) moiety between the donor and acceptor parts of coumarin dyes drastically improved the stability of the oxidized states in aqueous solution. The high stability of oxidized states enabled the dye molecules to work as durable sensitizers for stoichiometric production of $H_2$ and $I_3^-$ from aqueous solutions containing $I^-$ electron donor, when they were combined with an appropriate n-type semiconductor, layered niobate $H_4Nb_6O_{17}$.[24] Simultaneous evolution of $H_2$ and $O_2$ under visible light was thus achieved by combining the dye-adsorbed layered niobate with a $WO_3$ photocatalyst, which reduced the $I_3^-$ back to $I^-$ and oxidized water to $O_2$.

On the basis of these findings, we examined the influence of the molecular structure of dye, specifically that of the oligothiophene moiety, on both the stability in aqueous media and the efficiency of $H_2$ evolution in detail in the present study by using a series of coumarin and carbazole dyes. Additionally, nanoparticulate Pt inside the interlayer space of layered niobate and nanoparticulate $IrO_2$ coloaded with Pt on the surface of $WO_3$ were applied to improve the reaction selectivity toward $H_2$ and $O_2$ evolution, respectively, and their effects on efficiencies were examined in detail.

## 2. EXPERIMENTAL SECTION

**2.1. Preparation of $Pt/H_4Nb_6O_{17}$ Samples.** Crystals of ion-exchangeable layered niobium oxide ($K_4Nb_6O_{17}$) were prepared by


dx.doi.org/10.1021/ja4048637 | J. Am. Chem. Soc. 2013, 135, 16872−16884

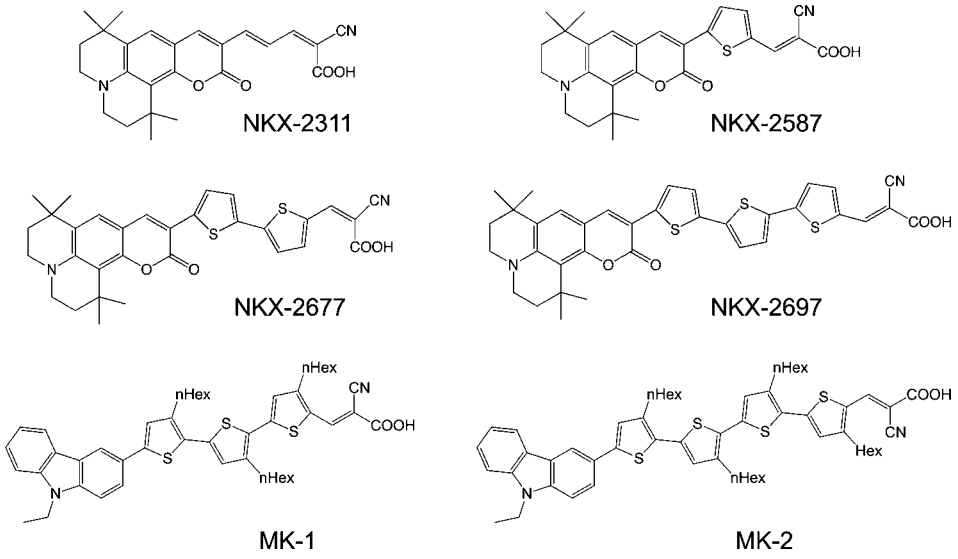


**Figure 2.** Molecular structures of dyes.

heating a stoichiometric mixture of $K_2CO_3$ and $Nb_2O_5$ in a platinum crucible at 1473 K for 15 min; the melt was rapidly cooled to room temperature. The polycrystalline $K_4Nb_6O_{17}$ produced was pulverized in an agate mortar to form a powder with particle sizes of 1−10 $\mu$m.[50] To introduce Pt nanoparticles (0.5 wt %) into the interlayer space, the $K_4Nb_6O_{17}$ particles were stirred in an aqueous solution containing the required amount of $[Pt(NH_3)_4]Cl_2$ for 3 days at room temperature. An appropriate amount of methanol was added to the aqueous solution (to be 10 vol %), which was then irradiated by a 300 W Xe lamp (Cermax LX-300F, $\lambda$ > 300 nm) for 12 h. In this process, the photoexcited electrons generated on the $K_4Nb_6O_{17}$ semiconductor reduced the $[Pt(NH_3)_4]^{2+}$ cations to metallic Pt, while the photogenerated holes oxidized methanol.[51] After being washed with distilled water several times, the sample was stirred in an aqueous HCl solution (0.5 M) for 72 h to exchange $K^+$ ions at the interlayers into $H^+$. Although an atomic absorption spectrometry indicated that only 60−75% of $K^+$ ions were exchanged to $H^+$ by this procedure, the proton-exchanged samples are referred to as $H_4Nb_6O_{17}$ hereafter for simplification. The prepared sample is thus referred to as Pt(in−out)/$H_4Nb_6O_{17}$, in which Pt metal particles exist mainly inside the interlayer spaces, as well as outside of the particles in part. Finally, the Pt(in−out)/$H_4Nb_6O_{17}$ sample was stirred in 3:1 concentrated HCl/$HNO_3$ at about 90 °C for 10 min to dissolve the Pt particles deposited on external sites of $H_4Nb_6O_{17}$ particles.[51] The material thus obtained is referred to as Pt(in)/$H_4Nb_6O_{17}$. A $TiO_2$ sample loaded with 0.5 wt % Pt was prepared as follows. A commercial $TiO_2$ powder (anatase, 320 $m^2\ g^{-1}$, Ishihara Co. Ltd., ST-01) was stirred in an aqueous methanol solution (10 vol %) containing the required amount of $H_2PtCl_6$ and irradiated by the Xe lamp for 12 h. After being washed with distilled water several times, the sample was heated at 473 K under a vacuum for 2 h to remove residual organic compounds.

**2.2. Adsorption of Dye Molecules on the Semiconductor Surface.** The coumarin dyes (NKX series)[35,37] used in the present study were provided by Hayashibara Biochemical Laboratories, Inc., Japan. The carbazole dyes (MK-1 and -2)[39] were synthesized as previously reported. The molecular structures of these dyes are shown in Figure 2. The Pt/$H_4Nb_6O_{17}$ or Pt/$TiO_2$ powder (0.5 g) was suspended in an acetonitrile−ethanol mixed solution (1:1 v/v, 50 mL) containing the NKX dye (0.3 mM) and stirred in the dark for 24 h. After separating the powder sample from the dye solution by centrifugation, it was washed once with an acetonitrile−ethanol solvent and twice by acetonitrile to remove superfluous dye molecules, and finally dried at room temperature and kept in a dark environment. In the case of MK dyes, a mixture of toluene and ethanol (1:1 v/v, 50 mL) was used as the solvent.

**2.3. Preparation of $IrO_2$ and Pt Coloaded $WO_3$ Photocatalyst.** A $WO_3$ powder (99.99%) was obtained from High Purity Chemical Co., Japan. Nanoparticulate Pt (0.5 wt %) cocatalyst was loaded onto the $WO_3$ particles by impregnation from aqueous $H_2PtCl_6$ solution, followed by calcination in air for 1 h at 773 K.[27] The obtained sample is referred to as Pt/$WO_3$, while it contains PtO along with Pt metal particle.[27] The $IrO_2$ (0.5 wt %) cocatalyst was then loaded on the Pt/$WO_3$ sample by impregnation from aqueous $Na_2IrCl_6$ solution followed again by calcination in air at 773 K for 1 h. This sample is referred to as $IrO_2$−Pt/$WO_3$. For comparison, sample loaded only with $IrO_2$ was prepared by the method described above, which will be referred to as $IrO_2$/$WO_3$.

**2.4. Electrochemical Measurements.** To examine the stability of dye molecules in aqueous solutions, their oxidation and reduction behaviors were analyzed by cyclic voltammetry (CV) in both aqueous and dehydrated acetonitrile (AN) solutions. Since all the dyes used in the present study are barely soluble in the aqueous solutions of pH lower than 7 due to their hydrophobic nature, their CV profiles in aqueous solutions could not be obtained by use of conventional techniques for the dissolved species. Thus, the CV measurements were carried out by using nanoporous $TiO_2$ electrodes adsorbed with the dye molecules.[52] Porous $TiO_2$ film electrodes were prepared by spreading a $TiO_2$ nanoparticle sol (Ishihara Co. Ltd., ST-21) on a conducting glass support (F-doped $SnO_2$). They were then calcined at 723 K for 30 min in air. The $TiO_2$ electrode was immersed in an acetonitrile−ethanol solution (1:1 v/v) of coumarin dye (0.3 mM) or in a toluene−ethanol solution (1:1 v/v) of carbazole dye (0.3 mM) and kept for more than 24 h at room temperature under dark conditions. The dye-adsorbed $TiO_2$ electrodes were washed with acetonitrile or toluene to remove superfluous dye molecules and then used immediately for the electrochemical measurements.

Electrochemical measurements were conducted with a potentiostat (Princeton Applied Research, PASTAT 2263) and a one-compartment cell consisting of a dye-adsorbed $TiO_2$ electrode, a Pt counter electrode, and a reference electrode. CV profiles of dye-adsorbed $TiO_2$ electrodes were examined in a dehydrated acetonitrile (AN) or aqueous solution, with a scan rate of 100 mV $s^{-1}$. Both the solutions contained 0.1 M $LiClO_4$ as a supporting electrolyte. As for the measurement in AN solutions, $Ag/Ag^+$ in 0.01 M $AgNO_3$/AN solution was used as a reference electrode, while Ag/AgCl in saturated aqueous NaCl solution was used as a reference in aqueous solutions. The solution was purged with argon gas for more than 30 min prior to the measurement.

**2.5. Photocatalytic Reactions.** Photocatalytic reactions were carried out using a Pyrex glass reactor connected to a closed gas-circulation system. In the case of $H_2$ evolution, the dye-adsorbed Pt/


dx.doi.org/10.1021/ja4048637 | J. Am. Chem. Soc. 2013, 135, 16872−16884

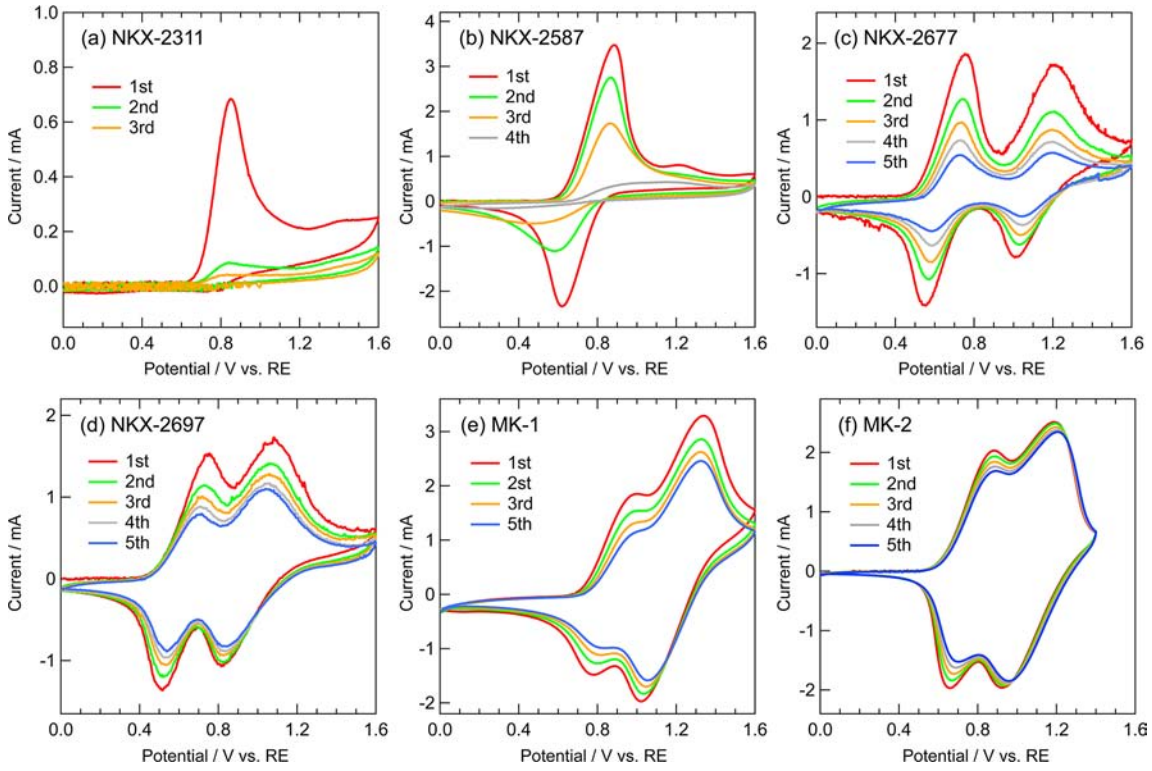


**Figure 3.** Wide range CV profiles of dyes adsorbed on a porous $TiO_2$ electrode in dehydrated acetonitrile containing 0.1 M $LiClO_4$ as a supporting electrolyte. The scan rate was 100 mV $s^{-1}$. $Ag/Ag^+$ in 0.01 M $AgNO_3$ acetonitrile solution was used as a reference electrode.

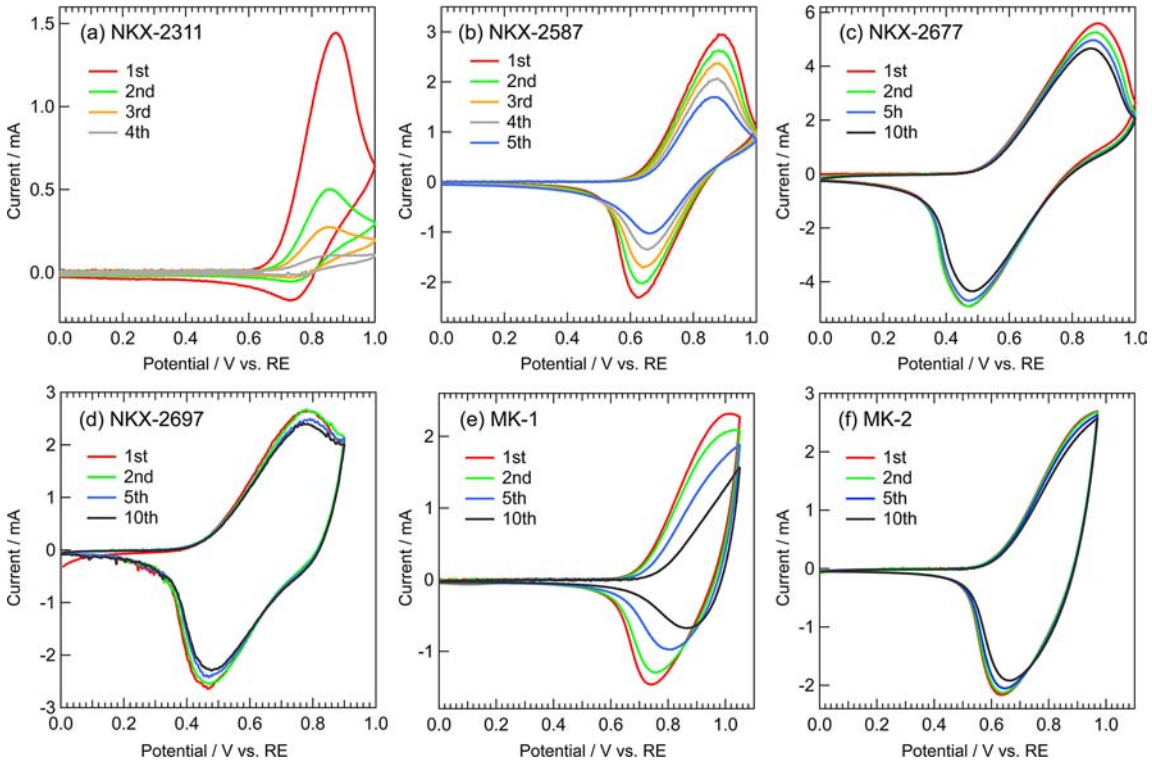


**Figure 4.** Narrow range CV profiles of dyes adsorbed on a porous $TiO_2$ electrode in dehydrated acetonitrile containing 0.1 M $LiClO_4$ as a supporting electrolyte. The scan rate was 100 mV $s^{-1}$. $Ag/Ag^+$ in 0.01 M $AgNO_3$ acetonitrile solution was used as a reference electrode.

$H_4Nb_6O_{17}$ (or $Pt/TiO_2$) photocatalyst powder (50 mg) was introduced into an aqueous potassium iodide (KI) solution (0.1 mol $L^{-1}$, 100 mL) in the reactor, and the suspension was stirred using a magnetic stir bar. Stirring the dye-adsorbed $Pt/H_4Nb_6O_{17}$ powder in the KI aq. (pH ~ 6.5, without adjustment) made the solution acidic (pH ~ 3.7) after 1 h, due to the cation exchange between $K^+$ in the solution and $H^+$ in the interlayers of $H_4Nb_6O_{17}$. In some cases, initial pH values of KI aq. were adjusted to be 1.0, 2.0, and 11.0 by adding appropriate amounts of $H_2SO_4$ or KOH, which were confirmed to be ca. 1.0, 2.0, and 9.0, respectively, after stirring the dye-adsorbed Pt/


dx.doi.org/10.1021/ja4048637 | J. Am. Chem. Soc. 2013, 135, 16872−16884

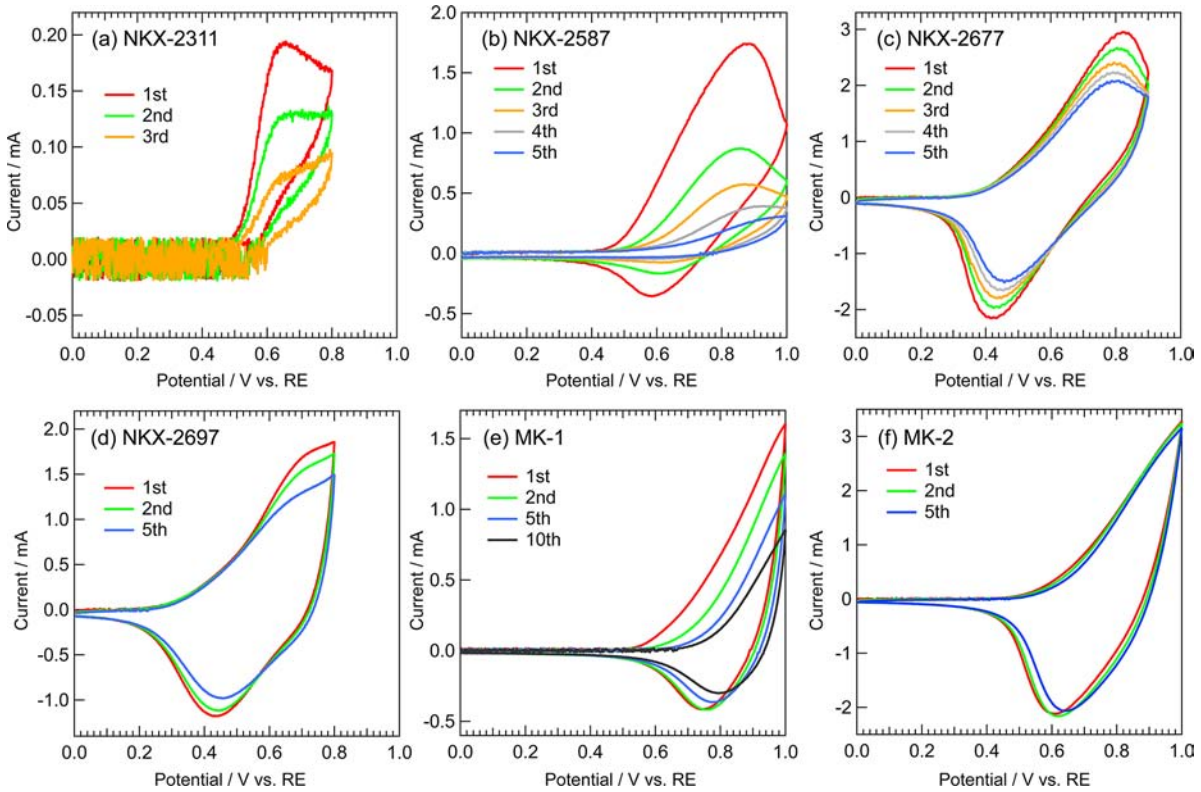


**Figure 5.** CV profiles of dyes adsorbed on a porous $TiO_2$ electrode in water containing 0.1 M $LiClO_4$ as a supporting electrolyte. The scan rate was 100 mV $s^{-1}$. Ag/AgCl in saturated aqueous NaCl solution was used as a reference electrode.

$H_4Nb_6O_{17}$ powder in each solution for 1 h. The system was thoroughly degassed by several cycles of evacuation and then introduced by Ar gas (ca. 13 kPa). The suspension was irradiated by visible light (410 nm < $\lambda$ < 800 nm) from the top of the reactor using the 300 W Xe lamp equipped with a UV-cut filter (Hoya L-42) and a cold mirror. In some cases, the reaction was carried out without any cutoff filters, in which both UV and visible light was irradiated ($\lambda$ > 300 nm). The reactor temperature was maintained at a constant value of 288 K during the reaction using cooling water. As for $O_2$ evolution, a $WO_3$ photocatalyst powder (100 mg) was suspended in an aqueous solution containing a fixed concentration of $KIO_3$ (2 mM) and various concentrations of KI (0−50 mM). In the case of overall water splitting, dye-adsorbed Pt/$H_4Nb_6O_{17}$ (50 mg) and $IrO_2$−Pt/$WO_3$ (100 mg) were mixed in an aqueous KI solution (5 mM), and then irradiated by visible light (410 nm < $\lambda$ < 800 nm). The evolved $H_2$ and/or $O_2$ gas was analyzed by an online gas chromatograph (TCD, molecular sieve 5 Å). The amount of $I_3^-$ ions generated in the aqueous solution after each reaction was determined on the basis of the absorption peak at around 350 nm, arising from $I_3^-$ anions.

## 3. RESULTS AND DISCUSSION

**3.1. Influence of the Oligothiophene Moiety on the Stability of Dye Molecules in Aqueous Media.** Dye molecules must be stable in their oxidized states, which are generated after the electron injection from the excited dye to a semiconductor (see Figure 1). This is indispensable for efficient regeneration of dye molecules and achieving steady $H_2$ evolution on dye-sensitized photocatalysts in an aqueous solution containing a reversible electron donor such as iodide ($I^-$). To examine the stability of dyes during the redox cycles, their oxidation and reduction behaviors were analyzed by cyclic voltammetry (CV) in both aqueous and dehydrated acetonitrile (AN) solutions. Since all the dyes used in the present study (see Figure 2) are barely soluble in the aqueous solutions of pH lower than 7 due to their hydrophobic natures and the acid dissociation constant of the carboxylic group, a nanoporous $TiO_2$ electrode adsorbed with the dye molecules was employed for the CV measurements.[52] When the potential on the $TiO_2$ electrode was scanned over a wide range from 0 to 1.6 V (vs reference, except for MK-2) in dehydrated acetonitrile (AN), one or two current peaks were observed due to the oxidation of dye molecules adsorbed on the $TiO_2$ surface (see Figure 3). The dye molecules having two or more thiophene rings (NKX-2677, NKX-2697, MK-1, and MK-2) exhibited two oxidation peaks in this scan range, as well as two corresponding reduction peaks in the reverse cathodic scan, indicating that these dye molecules can store two positive charges and can be reduced back to the original species by accepting two electrons within the lifetime in AN.

To estimate the stability of dye molecules during the dye-sensitized $H_2$ evolution (see Figure 1), in which one-electron processes are expected to predominate, scans in a narrower range were carried out in AN (Figure 4) and water (Figure 5) within the potential in which only one-electron oxidation−reduction takes place. A current peak corresponding to one-electron oxidation was observed during an anodic potential scan in all cases. On the other hand, the behavior during reverse cathodic scanning differed considerably depending on the structure of the dye molecule, specifically on the number of thiophene rings. For the coumarin NKX-2311 dye having no thiophene ring, no reduction peak was observed in water (Figure 5a), while a weak one was observed in AN (Figure 4a). Although the coumarin NKX-2587 dye having one thiophene ring exhibited almost reversible behavior in AN (Figure 4b), the intensity of the reduction peak in water was significantly lower than that of oxidation (Figure 5b). On the other hand, the


dx.doi.org/10.1021/ja4048637 | J. Am. Chem. Soc. 2013, 135, 16872−16884

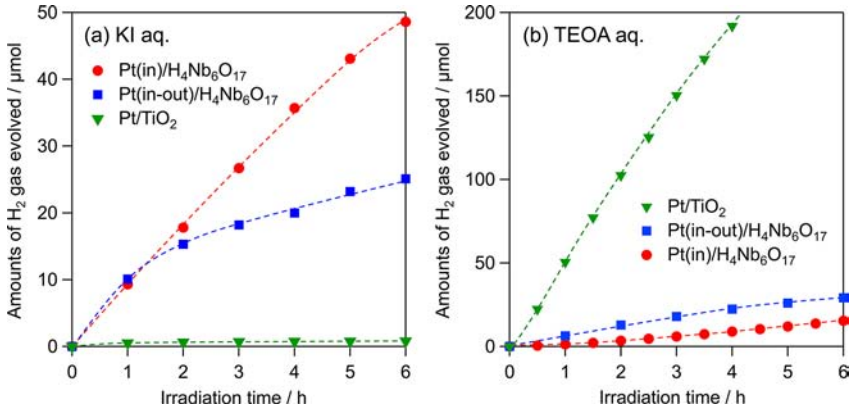


**Figure 6.** Time courses of photocatalytic $H_2$ evolution under visible light ($\lambda > 410$ nm) on NKX-2677 dye-adsorbed Pt(in)/$H_4Nb_6O_{17}$, Pt(in−out)/$H_4Nb_6O_{17}$, and Pt/$TiO_2$ photocatalysts suspended in (a) 0.1 M aqueous KI solution (pH ∼ 6.5, without adjustment) and (b) 0.1 M aqueous triethanolamine solution (pH ∼ 7, adjusted with HCl).

coumarin dyes having an oligothiophene moiety (i.e., two or more thiophene rings; NKX-2677 and NKX-2697) showed almost reversible behavior even in water (Figure 5c,d), as well as in AN (Figure 4c,d). This finding indicated that the one-electron oxidized states of these dyes have sufficiently long lifetimes even in water, and therefore can be reduced back to the original species by accepting an electron during the cathodic potential scan. For carbazole dyes, MK-2 with four thiophene rings exhibited almost reversible behavior even in water (Figure 5f), while MK-1 with three thiophene rings showed a rather irreversible CV profile in water (Figure 5e).

The repeated CV scans more clearly identified the influence of molecular structure on the stability. The intensities of oxidation peaks remarkably decreased with the increased number of scans for the coumarin dyes without oligothiophenes (NKX-2311, NKX-2587) in both AN and water. Since desorption of these dye molecules from the $TiO_2$ surface was negligible during the repeated CV scans, the decrease in peak intensity was undoubtedly due to the irreversible oxidation of dye molecules, generating some inactive species. For the coumarin dyes, the introduction of two or more thiophene rings (NKX-2677 and -2697) significantly improved the stability in both AN and water, while the intensities of oxidation peaks gradually decreased with increasing number of scans in both cases. For the carbazole system, the MK-2 dye having four thiophene rings showed much higher stability than the MK-1 dye that possesses three thiophene rings. Given the fact that a similar tendency was observed in both AN and water for all the dyes, the deactivation of dye molecules in AN was probably due to the irreversible reaction of the oxidized dyes with residual $H_2O$ molecules in AN. Clearly, introduction of two or more thiophene rings plays an essential role in stabilizing the one-electron oxidized states of dye molecules in aqueous media, while the carbazole system seems to require more thiophene rings than the coumarin one to be substantially stabilized.

**3.2. Photocatalytic $H_2$ Evolution from Water over Dye-Adsorbed Layered Niobate in the Presence of $I^-$ Electron Donor under Visible Light Irradiation.** These dyes were then used as photosensitizers of n-type semiconductors for $H_2$ evolution from an aqueous solution containing iodide ($I^-$) as an electron donor. However, the $H_2$ evolution from an aqueous KI (0.1 M) solution on a dye-adsorbed Pt/$TiO_2$, which is the best-known n-type semiconductor for dye sensitization, was found to readily terminate within a few hours of irradiation, with a tiny amount of $H_2$ gas evolved (see Figure 6a, for example). It was also confirmed that the $H_2$ evolution over dye-sensitized Pt/$TiO_2$ photocatalysts was entirely suppressed by adding a small amount of $I_3^-$ (ca. 50 $\mu$mol) into the solutions before photoirradiation. In contrast, the NKX-2677-adsorbed Pt/$TiO_2$ sample exhibited efficient $H_2$ evolution with a steady rate from an aqueous solution containing a sacrificial electron donor, triethanolamine (TEOA), as shown in Figure 6b. Clearly, a backward reaction, i.e., rereduction of $I_3^-$ to $I^-$, preferentially proceeded on the Pt cocatalysts loaded on $TiO_2$ in the presence of the $I_3^-/I^-$ redox couple, suppressing the $H_2$ evolution consequently (see Figure 7a).[49]

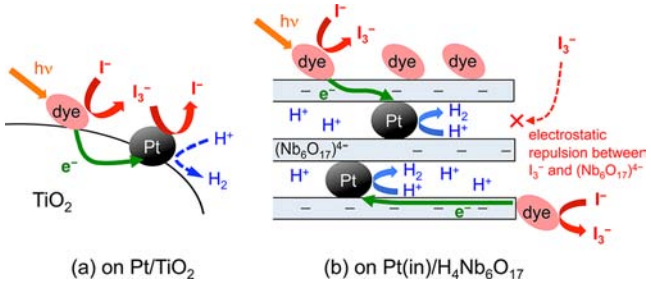


**Figure 7.** Conceptual schemes for suppression of backward reaction using nanostructured layered semiconductors.

In order to achieve steady $H_2$ evolution on the dye-sensitized systems, an internally platinized layered niobate, Pt(in)/$H_4Nb_6O_{17}$, was applied as an n-type semiconductor instead of Pt/$TiO_2$. It has been demonstrated that the use of Pt(in)/$H_4Nb_6O_{17}$, where Pt nanoparticles are selectively loaded in the interlayer spaces, is effective to suppress the undesirable backward reaction, i.e., rereduction of $I_3^-$ to $I^-$ on Pt.[45−47,49] As shown in Figure 6a, $H_2$ evolution proceeded with a steady rate over NKX-2677-adsorbed Pt(in)/$H_4Nb_6O_{17}$ from an aqueous solution containing an $I^-$ electron donor under visible light irradiation. Since $I_3^-$ anions are unable to access the Pt particles inside due to the electrostatic repulsion between the anionic $I_3^-$ and the negatively charged $(Nb_6O_{17})^{4-}$ layers, the backward reduction of $I_3^-$ to $I^-$ can be effectively suppressed (see Figure 7b).[45−47,49] When Pt cocatalysts were loaded both in the interlayers and on the outerlayers of $H_4Nb_6O_{17}$ [Pt(in−out)/$H_4Nb_6O_{17}$], the rate of $H_2$ evolution gradually decreased,


dx.doi.org/10.1021/ja4048637 | J. Am. Chem. Soc. 2013, 135, 16872−16884

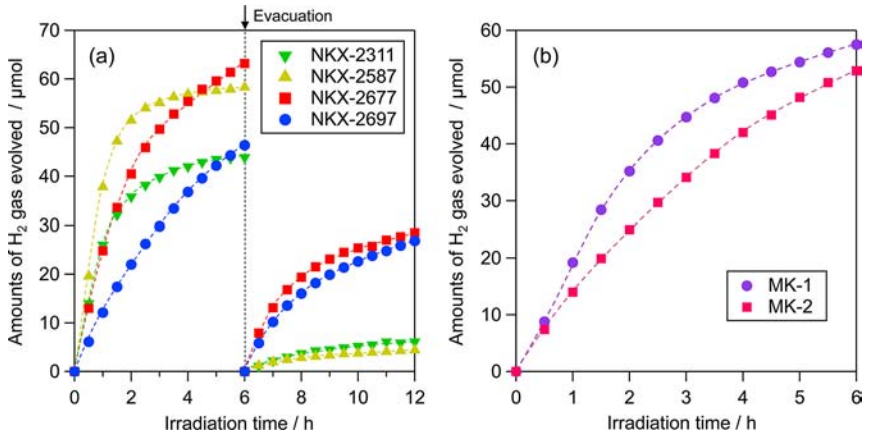


**Figure 8.** Time courses of photocatalytic $H_2$ evolution under visible light on dye-adsorbed Pt(in)/$H_4Nb_6O_{17}$ photocatalysts suspended in 0.1 M aqueous KI solution (initial pH ~ 3.7).

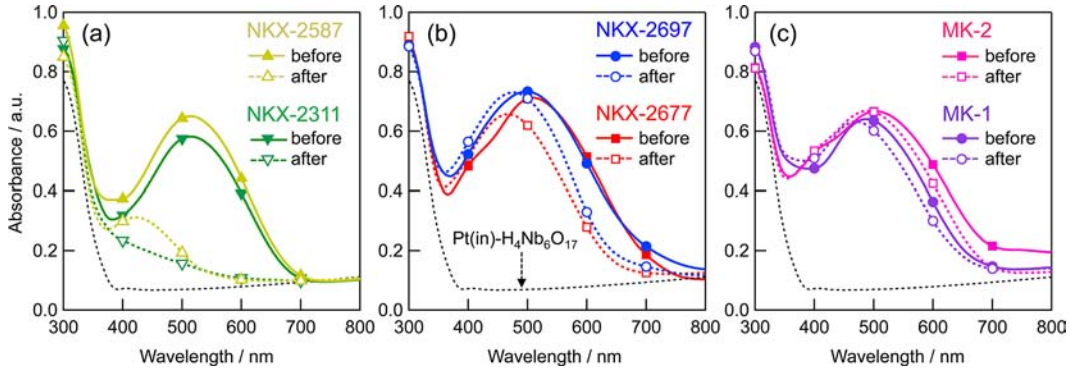


**Figure 9.** Diffuse reflectance spectra of dye-adsorbed Pt(in)−$H_4Nb_6O_{17}$ photocatalysts before and after the reactions shown in Figure 8.

undoubtedly due to the occurrence of backward reduction of $I_3^-$ on the outer Pt particles.

On the other hand, the dye-adsorbed Pt/$TiO_2$ photocatalyst exhibited a much higher rate of $H_2$ evolution than the dye-adsorbed Pt/$H_4Nb_6O_{17}$ samples in an aqueous TEOA solution, in which the occurrence of backward reaction can be neglected. The high rate of $H_2$ evolution is certainly due to both the much higher amount of adsorbed dye molecules (ca. 12 $\mu$mol/50 mg) and the efficient electron transfer from excited dye to Pt through the conduction band of $TiO_2$. The dye-adsorbed Pt(in)/$H_4Nb_6O_{17}$ system generated the lowest $H_2$, implying that the efficiency of electron transfer in the system is still insufficient due to the long distance between the dye molecules outside and Pt cocatalysts inside of interlayers. Since the $K_4Nb_6O_{17}$ particles prepared by solid state reaction possess relatively large particle sizes from several to a hundred $\mu$m,[50] it appears that only the Pt cocatalysts loaded in the interlayers near the outer surface mainly scavenge the electrons from dye molecules outside. The apparent quantum efficiency for $H_2$ production on NKX-2677-adsorbed Pt(in)/$H_4Nb_6O_{17}$ was determined to be ca. 0.05% at 480 nm under similar reaction conditions to those in Figure 6a, except for the light intensity of monochromatic light passed through a bandpass filter. Although the efficiency should be further improved by controlling the sizes or shapes of $K_4Nb_6O_{17}$ particles, the steady $H_2$ evolution on dye-adsorbed Pt(in)/$H_4Nb_6O_{17}$ samples allows us to evaluate the influence of dye structure on the stability and efficiency of $H_2$ evolution from water using an $I^-$ electron donor.

**3.3. Influence of Dye Structure on Photocatalytic $H_2$ Evolution from Water over Dye-Adsorbed Layered Niobate in the Presence of $I^-$ under Visible Light Irradiation.** Figure 8 shows the time courses of $H_2$ evolution over the dye-adsorbed layered niobate [Pt(in)/$H_4Nb_6O_{17}$] photocatalysts suspended in an aqueous KI solution (0.1 M, initial pH ~ 3.7) under visible light irradiation (410 nm < $\lambda$ < 800 nm). The rates of $H_2$ evolution on the Pt(in)/$H_4Nb_6O_{17}$ adsorbed by the coumarin dyes without oligothiophenes (NKX-2311 and NKX-2587) gradually decreased with irradiation time and became quite low after 6 h of irradiation (see the second runs after evacuation of the gas phase), while the initial rates of $H_2$ evolution were relatively high. The diffuse reflectance spectra of these samples markedly changed during the photoirradiation, as shown in Figure 9a, in which the absorption of dye molecules in the visible region (400−700 nm) was mostly disappeared after each reaction. Such a marked change was not observed when the photocatalysts were stirred in an aqueous KI solution in the dark, even under slightly basic conditions. This fact indicates that the marked decrease in absorption was caused by photochemical processes, not by the desorption of dye molecules from the Pt(in)/$H_4Nb_6O_{17}$ surface. A part of the oxidized state of dye molecules must have reacted with $H_2O$ molecules to form photoinactive species before accepting an electron from $I^-$ for regeneration, decreasing the number of active dye molecules gradually during the photoirradiation, as suggested by the results on electrochemical measurement for these dyes.


dx.doi.org/10.1021/ja4048637 | J. Am. Chem. Soc. 2013, 135, 16872−16884

**Table 1. Absorption and Electrochemical Properties of Coumarin and Carbazole Dyes**

| dye | $\lambda_{max}$[a] (nm) ($\varepsilon$, $M^{-1}$ $cm^{-1}$) | $\lambda_{max}$ (nm) (on $H_4Nb_6O_{17}$) | $E_{ox}$[b] (V) vs $Ag/Ag^+$ | $E_{ox}$[c] (V) vs SHE | initial rate of $H_2$ generation ($\mu$mol $h^{-1}$) |
|---|---|---|---|---|---|
| NKX-2311 | 483 (43500) | 516 | 0.81 | | 28.0 |
| NKX-2587 | 493 (54500) | 516 | 0.75 | 1.06 | 37.8 |
| NKX-2677 | 483 (60100) | 510 | 0.66 | 0.96 | 24.8 |
| NKX-2697 | 493 (70000) | 496 | 0.63 | 0.93 | 12.1 |
| MK-1 | 480 (38800) | 490 | 0.88 | | 19.2 |
| MK-2 | 480 (38400) | 503 | 0.77 | | 14.0 |

[a] $\lambda_{max}$ and the corresponding $\varepsilon$ were obtained from acetonitrile−ethanol mixed solutions (1:1 v/v) containing NKX dyes or toluene−ethanol mixed solutions (1:1 v/v) containing MK dyes. [b] Estimated from the reversible CV profiles in AN shown in Figures 3 and 4. [c] Estimated from the reversible CV profiles in aqueous solution shown in Figure 5, and then corrected to the potential vs SHE.

On the other hand, relatively steady $H_2$ evolution proceeded over the dyes with an oligothiophene (NKX-2677, NKX-2697, MK-1, and MK-2), as shown in Figure 8, and nearly the same amounts of $I_3^-$ as $H_2$ were detected in the solutions after all the reactions. The absorption of these dye molecules in the visible region can be clearly seen even after each reaction (see Figure 9b and c), while the absorption edges shifted to a shorter wavelength in all the cases, especially in the case of NKX-2677. The blue shift was probably caused by partial desorption of dye molecules from the $Pt(in)/H_4Nb_6O_{17}$ surface due to the pH change during the reaction, as well as by the progress of oxidative decomposition in part, which will be discussed in the next section. These findings indicated that the following reaction cycle took place continuously under visible light on the $Pt(in)/H_4Nb_6O_{17}$ adsorbed with the dyes having an oligothiophene moiety:

$$S + h\nu\ (\lambda > 400\ nm) \rightarrow S^*\ (\text{excitation of dye}) \quad (1)$$

$$S^* \rightarrow S^+ + e^-\ (\text{electron injection to } H_4Nb_6O_{17}) \quad (2)$$

$$2e^- + 2H^+ \rightarrow H_2\ (H_2 \text{ production on Pt}) \quad (3)$$

$$2S^+ + 2I^- \rightarrow 2S + I_2\ (\text{regeneration of dye}) \quad (4)$$

$$I_2 + I^- \rightarrow I_3^-\ (\text{generation of } I_3^-) \quad (5)$$

$$2H^+ + 3I^- \rightarrow H_2 + I_3^-\ (\text{total}) \quad (6)$$

These photocatalysis results again indicate the essential role of the oligothiophene moiety in stabilizing the oxidized state of dye molecules during the redox cycle in aqueous solutions. It should be noted that the electrochemical experiments (shown in Figures 3−5) were carried out under quite severe conditions, i.e., in the absence of an electron donor for regeneration, increasing the probability of deactivation through the reaction of the oxidized states with $H_2O$ molecules. On the other hand, the regeneration of dye molecules can take place competitively with the deactivation in the photocatalytic reactions carried out in the presence of a considerably high concentration of $I^-$ electron donor (0.1 M KI). Therefore, even the electrochemically unstable coumarin dyes that possess no oligothiophene moiety (NKX-2311 and -2587) could generate $H_2$ in the initial period, as seen in Figure 8a, while the activity decreased remarkably with prolonged irradiation time due to the occurrence of competitive deactivation of the dyes. As indicated by the electrochemical experiments, the oxidation states of dyes with an oligothiophene moiety possess sufficiently long lifetimes even in aqueous solutions, enabling the dye molecules to be regenerated by accepting an electron from $I^-$ and thus to work stably as photosensitizers for $H_2$ evolution.

Kato et al. examined the influence of the oligothiophene moiety on the stability of these coumarin and carbazole dyes adsorbed on nanocrystalline $TiO_2$ films under photoirradiation in air.[53] It was found that the dyes having an oligothiophene moiety between their donor and acceptor parts are much more robust than those without an oligothiophene moiety. The transient absorption spectra of the oxidized state of dyes indicated that the positive charge generated after electron injection localized within the oligothiophene moiety, regardless of the structure of the donor portion (i.e., coumarin or carbazole). Therefore, it is likely that the positive charge localized within the oligothiophene moiety possesses relatively low reactivity toward $H_2O$ molecules, while it can react with $I^-$ anions in the aqueous solution, enabling the regeneration by accepting an electron from $I^-$. The higher stability under ambient condition also implied that the dyes with an oligothiophene moiety are resistant to $O_2$ molecules, not only to $H_2O$. Indeed, the $Pt(in)/H_4Nb_6O_{17}$ adsorbed with the dye molecules having an oligothiophene moiety stably evolved $H_2$ even when the reaction was initiated in the presence of a considerable amount of $O_2$ in the gas phase. On the other hand, the positive charge generated in the dye molecules without an oligothiophene tend to delocalize over the whole $\pi$-conjugation system, and readily reacted with $H_2O$ and/or $O_2$ molecules, resulting in a loss of light absorption in the visible light region due to the destruction of $\pi$-conjugation.

Table 1 summarizes the properties of dyes together with the initial rate of $H_2$ evolution (determined from the results in Figure 8). The number of thiophene rings does not significantly affect the absorption properties of these dyes both in solution and on $H_4Nb_6O_{17}$. The oxidation potentials ($E_{ox}$), which correspond to the HOMO level, of these dyes were estimated from the reversible CV profiles shown in Figures 3−5. All the $E_{ox}$ values in acetonitrile (AN) solvent could be determined, while those in water could be determined only for NKX-2587, -2677, and -2697 dyes. The $E_{ox}$ values of coumarin dyes in AN clearly decreased with increasing numbers of thiophene rings: from 0.81 V (NKX-2311) to 0.63 V (NKX-2697). The $E_{ox}$ in water also decreased from 1.06 V (NKX-2587) to 0.93 V (NKX-2697). The same trend was observed for carbazole dyes (MK-1 and MK-2). In each dye system (except for NKX-2311), the initial rate of $H_2$ evolution decreased with increasing numbers of thiophene rings. These findings strongly suggested that inserting more thiophene rings lowers the efficiency in electron injection from $I_3^-/I^-$ (+0.54 V vs SHE) to the HOMO level due to the decreased energy gap between them, resulting in the lowered rate of $H_2$ evolution. The reduction potential ($E_{red}$), which corresponds to the LUMO levels, could be estimated on the basis of the $E_{ox}$ and energy gap of each dye. For example, the $E_{red}$ of NKX-2677 was estimated to be ca.


dx.doi.org/10.1021/ja4048637 | J. Am. Chem. Soc. 2013, 135, 16872−16884

−1.47 and −0.87 V vs SHE in aqueous solutions using the $\lambda_{max}$ value on $H_4Nb_6O_{17}$ (ca. 510 nm) and the $\lambda$ at absorption edge (ca. 700 nm), respectively. Even the later value (−0.87 V) seems to be sufficient for the electron injection from the LUMO level to the conduction band bottom of $H_4Nb_6O_{17}$, which was estimated to be ca. −0.27 V vs SHE.[46] Despite the increase in the energy gaps between the estimated $E_{red}$ and the conduction band bottom with increasing numbers of thiophene rings, the rate of $H_2$ evolution decreased. These facts strongly suggested that the energy gaps between the LUMO and conduction band bottom affected the efficiency of $H_2$ evolution less than those between the HOMO and $I_3^-/I^-$ redox.

From these results, we can conclude that the introduction of more thiophene rings significantly improves the stability of dye molecules during the redox cycle in aqueous solutions, while it lowers the rate of $H_2$ evolution probably due to the decreased efficiency in the electron injection from $I_3^-/I^-$ to HOMO. However, one cannot still exclude the possibility that other factors, such as structural difference in the main part of dye molecules (coumarin or calbazole) or geometric effect of oligothiophene, dominantly affect the efficiency of $H_2$ evolution. For example, MK-2 showed a lower rate of $H_2$ evolution than NKX-2677, despite the higher $E_{ox}$ potential. One possible explanation is that inserting more thiophene rings between the donor and acceptor parts lowers the efficiency in electron transfer from the dye to the semiconductor through the longer oligothiophene moiety. More systematic investigation is required to clarify the influence of each factor on the overall efficiency.

**3.4. Influence of pH Values and Irradiation Wavelength on Photocatalytic $H_2$ Evolution.** Figure 10 shows

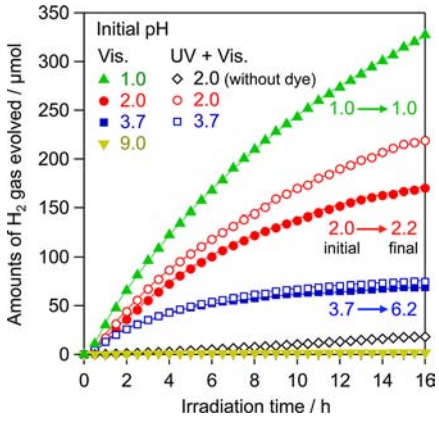


**Figure 10.** Time courses of $H_2$ evolution over NKX-2677-adsorbed Pt(in)/$H_4Nb_6O_{17}$ photocatalysts suspended in aqueous KI solutions with different pH values under full arc (UV + Vis; 300 nm < $\lambda$ < 800 nm) or visible light (410 nm < $\lambda$ < 800 nm) irradiation.

the time courses of $H_2$ evolution over NKX-2677-adsorbed Pt(in)/$H_4Nb_6O_{17}$ photocatalysts suspended in aqueous KI solutions with different pH values. In some cases, reactions were carried out under full arc irradiation from the Xe lamp, which includes both UV and visible light ($\lambda$ > 300 nm), in order to investigate the influence of UV light that induces direct excitation of $H_4Nb_6O_{17}$ (ca. 380 nm of absorption edge) on both the activity and stability. As described in the Experimental Section, the pH value of nonadjusted KI aq. was confirmed to change from 6.5 to ∼3.7 by stirring the dye-adsorbed Pt(in)/$H_4Nb_6O_{17}$ powder (50 mg) in the solution for 1 h. This change is due to the cation exchange between $K^+$ in the solution and $H^+$ contained in the interlayers of $H_4Nb_6O_{17}$. When the reaction was initiated at pH 3.7 without pH adjustment, in the same manner as in Figure 8, the rate of $H_2$ evolution gradually decreased with irradiation time and became quite low after 10 h of irradiation, as shown in Figure 10. Because the $H_2$ evolution from water with $I^-$ electron donor consumes $H^+$ in the progress of reaction (see eq 6), the pH value actually increased from 3.7 to ∼6.2 during the reaction (see Figure 10). Therefore, the lack of $H^+$ in the reaction media probably caused the decrease in the rate of $H_2$ evolution when the reaction was initiated without pH adjustment. Indeed, such a decrease was effectively suppressed by applying lower pH conditions. As shown in Figure 10, relatively steady $H_2$ evolution with higher rates was observed in acidic solutions (pH 1 or 2). On the other hand, $H_2$ evolution was negligible in a basic KI solution (pH 9). Figure 11 shows

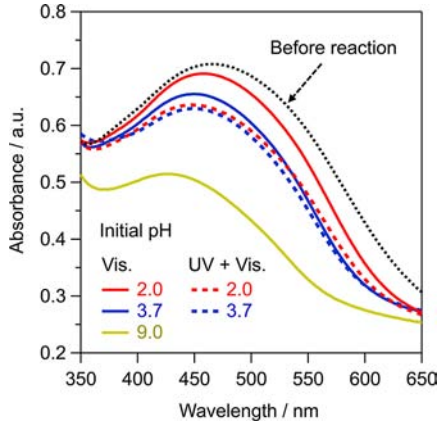


**Figure 11.** Diffuse reflectance spectra of NKX-2677-adsorbed Pt(in)−$H_4Nb_6O_{17}$ photocatalysts before and after the reaction shown in Figure 10.

the diffuse reflectance spectra of NKX-2677-adsorbed Pt(in)−$H_4Nb_6O_{17}$ photocatalysts before and after the reactions. The absorption in visible region apparently decreased and shifted to a shorter wavelength after the reaction in unadjusted aqueous KI solution (pH 3.7). Such change in absorption was clearly suppressed by applying lower pH conditions, (pH 2). Since these dyes possess a carboxylic acid group as an anchor to semiconductor surface, they can be soluble in a basic aqueous solution. Indeed the reaction at pH 9 resulted in the significant decrease in absorption (see Figure 11), undoubtedly due to desorption of dye molecules during the reaction. It therefore appears that a part of dye molecules desorbed from the surface of Pt(in)/$H_4Nb_6O_{17}$ due to the increased pH value in the progress of $H_2$ evolution when the reaction was initiated without pH adjustment (pH 3.7).

The full arc irradiation, which includes both UV and visible light, to the NKX-2677-adsorbed Pt(in)/$H_4Nb_6O_{17}$ photocatalyst appreciably enhanced the $H_2$ evolution, as clearly seen in the reaction at pH 2. The bare Pt(in)/$H_4Nb_6O_{17}$ sample without dye adsorption was found to generate appreciable $H_2$ from an aqueous KI solution (pH 2) under the full arc irradiation (see Figure 10), suggesting partial contribution of direct excitation of $H_4Nb_6O_{17}$ to the $H_2$ evolution on the dye-absorbed samples. However, the full arc irradiation obviously decreased the absorption of dyes after the reaction (see Figure 11), indicating the oxidative degradation of dye molecules by the holes generated on $H_4Nb_6O_{17}$. It can be therefore


dx.doi.org/10.1021/ja4048637 | J. Am. Chem. Soc. 2013, 135, 16872−16884

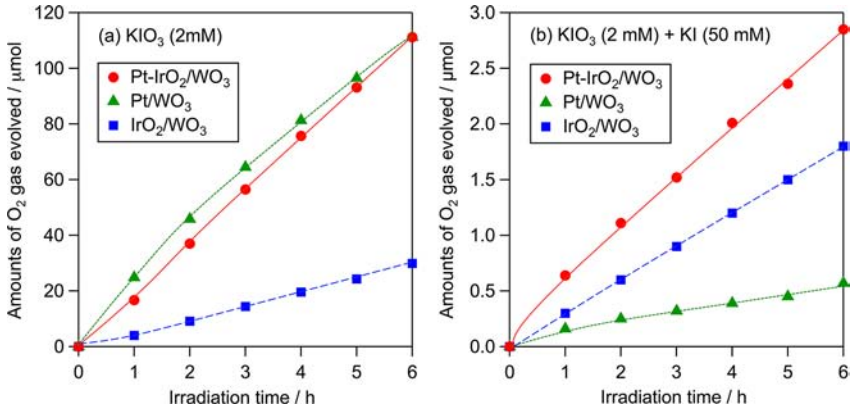


**Figure 12.** Time courses of photocatalytic $O_2$ evolution under visible light irradiation over various $WO_3$ photocatalysts suspended in aqueous solutions (250 mL, pH ~ 6 without adjustment) containing (a) 2 mM of $KIO_3$ and (b) 2 mM of $KIO_3$ and 50 mM of KI.

concluded that the light in the UV region should be eliminated to avoid the deactivation of dye molecules and to achieve stable $H_2$ evolution on dye-adsorbed Pt(in)/$H_4Nb_6O_{17}$ photocatalyst.

**3.5. Oxidation of Water to $O_2$ over Cocatalyst-Loaded $WO_3$ Photocatalysts.** As described above, some dye-adsorbed Pt(in)/$H_4Nb_6O_{17}$ photocatalysts could stably evolve $H_2$ from an aqueous solution containing $I^-$, accompanied by generation of $I_3^-$ as an oxidized product from $I^-$. For achieving overall water splitting (i.e., simultaneous evolution of $H_2$ and $O_2$) using these dye-sensitized photocatalysts, it is necessary to develop the $O_2$-evolving photocatalyst that can evolve $O_2$ from aqueous solution containing $I_3^-$. Additionally, the $O_2$-evolving photocatalyst must be capable of evolving $O_2$ even in the presence of a relatively high concentration of $I^-$, which is required for the effective regeneration of the oxidized state of dye molecules (eq 4). However, it has been proven that the rate of $O_2$ evolution on tungsten oxide ($WO_3$), which is known as one of the efficient $O_2$-evolving photocatalysts, significantly decreases with increasing concentration of $I^-$, due to the occurrence of competitive oxidation of $I^-$ by holes on the surface of $WO_3$.[27] Thus, loading of various $O_2$-evolving cocatalysts on $WO_3$ particles was attempted to improve the selectivity of holes toward the oxidation of water.

Since the main oxidized product on the dye-adsorbed Pt(in)/$H_4Nb_6O_{17}$ photocatalysts was $I_3^-$, the $O_2$ evolution activity of $WO_3$ photocatalysts should be evaluated using $I_3^-$ as an electron acceptor. However, both the insufficient solubility of iodine ($I_2$) in aqueous KI solution ($I_2 + I^- \rightarrow I_3^-$) and the relatively high volatility of $I_2$ prevented the preparation of reaction solutions containing appropriate amounts of $I_3^-$, especially when the concentrations of $I^-$ were low. Furthermore, the light absorption of $I_3^-$ in the visible light region disturbed the accurate evaluation of the $O_2$ evolution rate under visible light irradiation. Iodate anion ($IO_3^-$) with light absorption shorter than 300 nm was thus used as an electron acceptor instead of $I_3^-$, since it has a similar redox potential ($IO_3^-/I^-$: +0.67 V vs SHE at pH 7) to that of $I_3^-/I^-$ (+0.54 V vs SHE at pH 7) and sufficiently high solubility in aqueous solutions.[13,31]

Figure 12 shows time courses of photocatalytic $O_2$ evolution on Pt-loaded $WO_3$, $IrO_2$-loaded $WO_3$, and $IrO_2$–Pt-coloaded $WO_3$ photocatalysts suspended in aqueous solutions containing $IO_3^-$ alone or containing both $IO_3^-$ and $I^-$. Although the Pt–$IrO_2/WO_3$ and Pt/$WO_3$ samples showed almost comparable activity in the absence of $I^-$ (see Figure 12a), Pt–$IrO_2/WO_3$ exhibited much higher activity than Pt/$WO_3$ in the copresence of $I^-$ (50 mM) and $IO_3^-$. The lower activity of $IrO_2/WO_3$ (see Figure 12a) is undoubtedly due to the lack of reduction sites for the reduction of $IO_3^-$ in a six-electron process.[13,27] Figure 13 shows the rates of $O_2$ evolution on these photocatalysts in aqueous solutions containing a fixed concentration of $IO_3^-$ (2 mM) and different concentrations of $I^-$ (0–50 mM). Although the rates of $O_2$ evolution drastically decreased with increasing concentration of $I^-$ both on Pt/$WO_3$ and Pt-$IrO_2/WO_3$, the degree of the decrease on Pt–$IrO_2/WO_3$ was clearly less, resulting in higher rates of $O_2$ evolution on Pt–$IrO_2/WO_3$ with $I^-$ concentrations above 2 mM than those on Pt/$WO_3$. These results strongly suggested that some holes generated in $WO_3$ migrated to the $IrO_2$ cocatalyst, which is known to be an effective water-oxidation catalyst,[54] and oxidizes water to $O_2$ with higher selectivity than on the bare $WO_3$ surface.

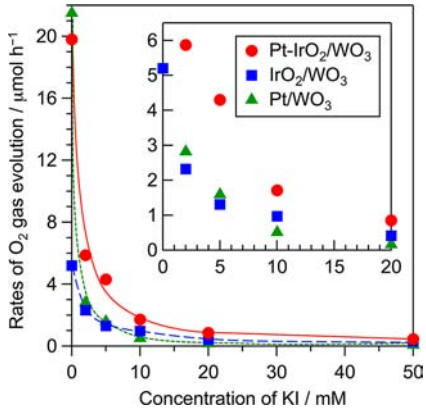


**Figure 13.** Rates of $O_2$ evolution over $WO_3$ photocatalysts in aqueous solutions containing different concentrations of $I^-$ (0–50 mM) and a fixed concentration of $IO_3^-$ (2 mM).

**3.6. Simultaneous Evolution of $H_2$ and $O_2$ under Visible Light Irradiation Using a Combination of Dye-Adsorbed Pt(in)/$H_4Nb_6O_{17}$ and $WO_3$ Photocatalysts.** Water splitting under visible light was then tried by combining the dye-adsorbed Pt(in)/$H_4Nb_6O_{17}$ photocatalysts with the $WO_3$ photocatalysts. The combination of NKX-2677–Pt(in)/$H_4Nb_6O_{17}$ and Pt–$IrO_2/WO_3$ allowed steady evolution of $H_2$ and $O_2$ in a nearly stoichiometric ratio ($H_2$, 14.1 $\mu$mol; $O_2$, 6.8 $\mu$mol at 8 h), as shown in Figure 14. The use of Pt/$WO_3$ resulted in a smaller amount of $O_2$ than the stoichiometric


dx.doi.org/10.1021/ja4048637 | J. Am. Chem. Soc. 2013, 135, 16872–16884

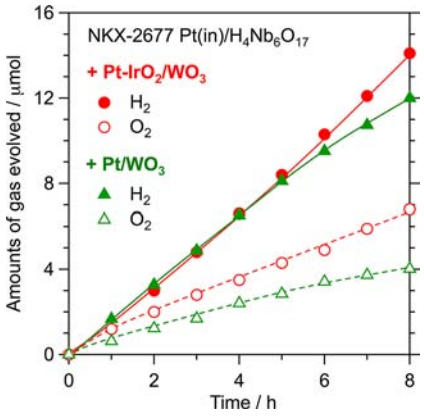


**Figure 14.** Time courses of photocatalytic evolution of $H_2$ and $O_2$ using a mixture of NKX-2677–$Pt/H_4Nb_6O_{17}$ (50 mg) and $WO_3$ (100 mg) photocatalysts suspended in 5 mM KI aqueous solution under visible light.

value ($H_2$, 12.0 $\mu$mol; $O_2$, 4.0 $\mu$mol at 8 h), with a gradual decrease in gas evolution rates after 5 h of irradiation. The deviation from stoichiometry is certainly due to the undesirable oxidation of $I^-$ to $I_3^-$ by the holes generated on $Pt/WO_3$, which possesses lower selectivity toward water oxidation than Pt–$IrO_2/WO_3$, as demonstrated in Figure 13. The decrease in the gas evolution rates in the $Pt/WO_3$ system is possibly due to the light shielding by $I_3^-$ generated on $Pt/WO_3$, since the accumulation of an appreciable amount of $I_3^-$ was confirmed in the solution after the reaction.

The rate of gas evolution increased with increasing $I^-$ concentration up to 5 mM but decreased significantly with further increase in concentration. The increase in gas evolution rate is undoubtedly due to the enhanced $H_2$ evolution on the NKX-2677–$Pt(in)/H_4Nb_6O_{17}$ photocatalyst by adding more $I^-$ electron donor, whereas the decreased rate at higher $I^-$ concentrations is certainly due to the enhanced rate of undesirable oxidation of $I^-$ over the Pt–$IrO_2/WO_3$ photocatalyst, which lowers the rate of $O_2$ evolution and also causes the accumulation of $I_3^-$. It was also confirmed that the ratio between dye-adsorbed $Pt(in)/H_4Nb_6O_{17}$ and Pt–$IrO_2/WO_3$ photocatalysts affected the ratio in $H_2/O_2$ evolved during the reaction; the optimal combinations were found to be 50 and 100 mg, respectively.

The activity of each dye for visible-light-induced water splitting was evaluated by irradiating the mixture of dye-adsorbed $Pt(in)/H_4Nb_6O_{17}$ (50 mg) with Pt–$IrO_2/WO_3$ (100 mg) in aqueous KI solution (5 mM, pH ~ 4.5 without adjustment). For the coumarin NKX-2311 dye without thiophene rings, only a small amount of $H_2$ evolved in the initial period and the gas evolution completely terminated within 8 h, as shown in Figure 15a. Although simultaneous evolution of $H_2$ and $O_2$ was observed in the initial period on the NKX-2587 system having one thiophene ring, the evolution rates significantly decreased with prolonged irradiation time, as Figure 15a shows. On the other hand, the use of NKX-2677 dye, which has two thiophene rings, allowed simultaneous evolution of $H_2$ and $O_2$ in nearly stoichiometric ratio even for long photoirradiation times, while the rates of gas evolution appreciably decreased after 40 h of irradiation. The total amount of evolved $H_2$ for 64 h (ca. 141.0 $\mu$mol) exceeded the amount of dye molecules adsorbed on $Pt(in)/H_4Nb_6O_{17}$ (ca. 0.55 $\mu$mol), giving a turnover number of ca. 513 (see Table 2).

**Table 2. Photocatalytic Activities of Dye-Adsorbed $Pt/H_4Nb_6O_{17}$ Combined with $IrO_2$–$Pt/WO_3$ Photocatalyst from Aqueous KI Solution under Visible Light Irradiation[a]**

| dye | amount of dye[b] ($\mu$mol) | irradiation time (h) | amount of gas evolved ($\mu$mol) $H_2$ | amount of gas evolved ($\mu$mol) $O_2$ | TON for $H_2$ evolution[c] |
|---|---|---|---|---|---|
| NKX-2311 | 0.51 | 8 | 0.6 | 0 | 2.4 (8 h) |
| NKX-2587 | 0.50 | 24 | 23.8 | 10.1 | 95 (24 h) |
| NKX-2677 | 0.55 | 24 | 50.4 | 21.3 | 183 (24 h) |
| | | 64 | 141.0 | 59.1 | 513 (64 h) |
| NKX-2697 | 0.52 | 24 | 26.9 | 12.3 | 104 (54 h) |
| | | 64 | 82.3 | 35.1 | 317 (64 h) |
| MK-1 | 0.71 | 24 | 26.4 | 10.2 | 75 (24 h) |
| MK-2 | 0.56 | 24 | 40.3 | 15.8 | 144 (24 h) |

[a]Reaction conditions: catalyst, 50 mg of dye-adsorbed Pt (in, 0.5 wt %)/$H_4Nb_6O_{17}$ and 100 mg of $IrO_2$ (0.5 wt %)–Pt (0.5 wt %)/$WO_3$; aqueous KI solution (5 mM, 100 mL); light source, xenon lamp (300 W) fitted with L-42 cutoff filter; reaction vessel, Pyrex top-irradiation type; irradiation wavelength, 410 nm < $\lambda$ < 800 nm. [b]Amount of dye molecules adsorbed on 50 mg of $Pt/H_4Nb_6O_{17}$. [c]Calculated as follows: turnover number = amount of $H_2$ evolved × 2/amount of dye molecules adsorbed on 50 mg of $Pt/H_4Nb_6O_{17}$.

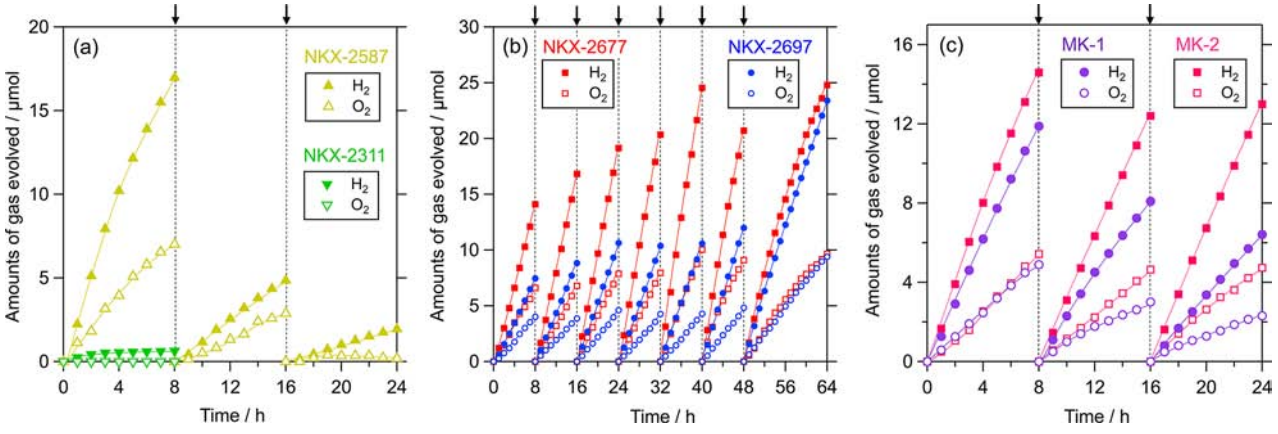


**Figure 15.** Time courses of $H_2$ (closed) and $O_2$ (open) evolution using a mixture of dye-adsorbed [(a) NKX-2311 and NKX-2587, (b) NKX-2677 and NKX-2697, and (c) MK-1 and MK-2] $Pt/H_4Nb_6O_{17}$ (50 mg) and $IrO_2$–$Pt/WO_3$ (100 mg) suspended in 5 mM KI aqueous solution (pH ~ 4.5, without adjustment) under visible light. Arrows indicate evacuation of gas phase.


dx.doi.org/10.1021/ja4048637 | J. Am. Chem. Soc. 2013, 135, 16872–16884

Simultaneous evolution of $H_2$ and $O_2$ was also observed for NKX-2697, with three thiophene rings, with steady rates even after 48 h of irradiation (see Figure 15b), while the initial rates of gas evolution were lower than those on NKX-2677 dye. These results again indicated that introducing more thiophene rings makes the dye molecules more robust during the redox cycle in aqueous solutions, while it lowers the efficiency in $H_2$ evolution, as discussed in a previous section. Although both the carbazole systems (MK-1 and MK-2) exhibited simultaneous evolution of $H_2$ and $O_2$, the rate of gas evolution on the MK-1 system gradually decreased, as seen in Figure 15c, indicating that the introduction of four thiophene rings (MK-2) is required for substantial stabilization of the carbazole dye system, agreeing well with the results on the electrochemical measurements.

Table 2 summarizes the results on water splitting using the combinations of dye-adsorbed Pt(in)/$H_4Nb_6O_{17}$ and Pt−$IrO_2$/$WO_3$ in aqueous KI solutions under visible light. The coumarin dyes having two or three thiophene rings (NKX-2677 and -2697), as well as the carbazole dye with four thiophene rings (MK-2), showed higher turnover numbers than the others. It should be noted here that these numbers were not the maximum values, since their activities still remained even at the end of the photoreactions (see Figure 15b and c). On the other hand, the turnover numbers for NKX-2311 and NKX-2587 seem to be close to the maximum values, since the rates of gas evolution became almost negligible at the end of the reactions. The activity of the MK-1 system also decreased gradually over a long irradiation time. These results again indicated that the insertion of the oligothiophene moiety is quite effective for stabilizing these dye molecules during photocatalytic water splitting, while the required number of thiophene rings is different between coumarin and carbazole systems.

The quantum efficiencies of the dye-sensitized $H_2$ evolution are quite low (e.g., ca. 0.05% at 480 nm for the NKX-2677 system) at present. One possible explanation for the low efficiency is the low efficiency in electron transfer from the dye molecules outside to the Pt cocatalysts inside through the micrometer sized $H_4Nb_6O_{17}$ particles. Another possible reason is the intrinsically low rate of electron injection from $I^-$ to dyes in aqueous media. Spiccia et al. have recently reported highly efficient aqueous dye-sensitized $TiO_2$ solar cells with the carbazole MK-2 dye in conjunction with electrolytes based on the $Fe(CN)_6^{4-/3-}$ redox couple in water, with incident photon to electron conversion efficiencies above 80%.[55] This high efficiency in aqueous media indicates the possibility for developing an efficient dye-sensitized water splitting system by employing an appropriate shuttle redox mediator other than $I_3^-/I^-$.

## 4. SUMMARY

We demonstrated Z-scheme-type water splitting under visible light using simple molecular sensitizers such as coumarin or carbazole dyes adsorbed on a layered niobate for the $H_2$ evolution part. It was revealed that the insertion of an oligothiophene (two or more thiophene rings) moiety between the donor and acceptor parts of these dyes effectively improves the stability of their oxidized states in aqueous solutions, certainly due to the localization of positive charge within the oligothiophene moiety that possesses low reactivity toward water molecules. This unique stabilizing ability of the oligothiophene moiety enabled us to achieve visible-light-induced water splitting using these robust dye sensitizers as $H_2$-evolving photocatalysts, combined with an effective $O_2$-evolving $IrO_2$−Pt/$WO_3$ photocatalyst through the redox cycle between $I_3^-$ and $I^-$. It will also provide us the chance to diversify the $H_2$-evolving photocatalysts available for the Z-scheme water-splitting systems by eliminating the difficulty in tailoring the band levels of inorganic semiconductors for $H_2$ evolution under visible light. Although the quantum efficiency of the dye-sensitized $H_2$ evolution is currently low, optimal design of organic dye molecules, as well as semiconductors, for efficient electron transfers in aqueous solutions will improve the efficiency and help us to achieve efficient water splitting harvesting a wide range of the solar light spectrum.

## AUTHOR INFORMATION


### Corresponding Author

ryu-abe@scl.kyoto-u.ac.jp

### Present Address

[‖]Graduate School of Engineering, Kyoto University, Katsura, Nishikyo-ku, Kyoto 615-8510, Japan.


### Notes

The authors declare no competing financial interest.

## ACKNOWLEDGMENTS

This work was supported by the JST PRESTO and the JSPS -NEXT programs.

## REFERENCES


(1) Bolton, J. R. *Sol. Energy* **1996**, *57*, 37−50.
(2) Domen, K.; Kondo, J. N.; Hara, M.; Takata, T. *Bull. Chem. Soc. Jpn.* **2000**, *73*, 1307−1331.
(3) Esswein, A. J.; Nocera, D. G. *Chem. Rev.* **2007**, *107*, 4022−4047.
(4) Osterloh, F. E. *Chem. Mater.* **2008**, *20*, 35−54.
(5) Kudo, A.; Miseki, Y. *Chem. Soc. Rev.* **2009**, *38*, 253−278.
(6) Inoue, Y. *Energy Environ. Sci* **2009**, *2*, 364−386.
(7) Kitano, M.; Hara, M. *J. Mater. Chem.* **2010**, *20*, 627−641.
(8) Abe, R. *J. Photochem. Photobiol., C* **2010**, *11*, 179−209.
(9) Maeda, K. *J. Photochem. Photobiol., C* **2011**, *12*, 237−268.
(10) Sayama, K.; Mukasa, K.; Abe, R.; Abe, Y.; Arakawa, H. *Chem. Commun.* **2001**, 2416−2417.
(11) Sayama, K.; Mukasa, K.; Abe, R.; Abe, Y.; Arakawa, H. *J. Photochem. Photobiol., A* **2002**, *148*, 71−77.
(12) Kato, H.; Hori, M.; Konta, R.; Shimodaira, Y.; Kudo, A. *Chem. Lett.* **2004**, *33*, 1348−1349.
(13) Abe, R.; Sayama, K.; Sugihara, H. *J. Phys. Chem. B* **2005**, *109*, 16052−16061.
(14) Abe, R.; Takata, T.; Sugihara, H.; Domen, K. *Chem. Commun.* **2005**, 3829−3831.
(15) Maeda, K.; Takata, T.; Hara, M.; Saito, N.; Inoue, Y.; Kobayashi, H.; Domen, K. *J. Am. Chem. Soc.* **2005**, *127*, 8286−8287.
(16) Maeda, K.; Teramura, K.; Lu, D.; Takata, T.; Saito, N.; Inoue, Y.; Domen, K. *Nature* **2006**, *440*, 295.
(17) Lee, Y.; Terashima, H.; Shimodaira, Y.; Teramura, K.; Hara, M.; Kobayashi, H.; Domen, K.; Yashima, M. *J. Phys. Chem. C* **2007**, *111*, 1042−1048.
(18) Kato, H.; Sasaki, Y.; Iwase, A.; Kudo, A. *Bull. Chem. Soc. Jpn.* **2007**, *80*, 2457−2464.
(19) Higashi, M.; Abe, R.; Ishikawa, A.; Takata, T.; Ohtani, B.; Domen, K. *Chem. Lett.* **2008**, *37*, 138−139.
(20) Higashi, M.; Abe, R.; Teramura, K.; Takata, T.; Ohtani, B.; Domen, K. *Chem. Phys. Lett.* **2008**, *452*, 120−123.
(21) Sasaki, Y.; Iwase, A.; Kato, H.; Kudo, A. *J. Catal.* **2008**, *259*, 133.
(22) Higashi, M.; Abe, R.; Takata, T.; Domen, K. *Chem. Mater.* **2009**, *21*, 1543−1549.
(23) Sasaki, Y.; Nemoto, H.; Saito, K.; Kudo, A. *J. Phys. Chem. C* **2009**, *113*, 17536−17542.

(24) Abe, R.; Shinmei, K.; Hara, K.; Ohtani, B. *Chem. Commun.* **2009**, 3577−3579.
(25) Tabata, M.; Maeda, K.; Higashi, M.; Lu, D.; Takata, T.; Abe, R.; Domen, K. *Langmuir* **2010**, *26*, 9161−9165.
(26) Maeda, K.; Higashi, M.; Lu, D.; Abe, R.; Domen, K. *J. Am. Chem. Soc.* **2010**, *132*, 5858−5869.
(27) Abe, R.; Higashi, M.; Domen, K. *ChemSusChem* **2011**, *4*, 228−237.
(28) Abe, R. *Bull. Chem. Soc. Jpn.* **2011**, *84*, 1000−1030.
(29) Sasaki, Y.; Kato, H.; Kudo, A. *J. Am. Chem. Soc.* **2013**, *135*, 5441−5449.
(30) Bard, A. J. *J. Photochem.* **1979**, *10*, 59−75.
(31) Abe, R.; Sayama, K.; Domen, K.; Arakawa, H. *Chem. Phys. Lett.* **2001**, *344*, 339−344.
(32) Scaife, D. E. *Sol. Energy* **1980**, *25*, 41−54.
(33) Hagberg, D. P.; Marinado, T.; Karlsson, K. M.; Nonomura, K.; Qin, P.; Boschloo, G.; Brinck, T.; Hagfeldt, A.; Sun, L. *J. Org. Chem.* **2007**, *72*, 9550−9556.
(34) Sayama, K.; Hara, K.; Mori, N.; Satsuki, M.; Suga, S.; Tsukagoshi, S.; Abe, Y.; Sugihara, H.; Arakawa, H. *Chem. Commun.* **2000**, *2000*, 1173−1174.
(35) Hara, K.; Sayama, K.; Ohga, Y.; Shinpo, A.; Suga, S.; Arakawa, H. *Chem. Commun.* **2001**, *2001*, 569−570.
(36) Horiuchi, T.; Miura, H.; Sumioka, K.; Uchida, S. *J. Am. Chem. Soc.* **2004**, *126*, 12218−12219.
(37) Hara, K.; Z. S. Wang, Z. S.; Sato, T.; Furube, A.; Katoh, R.; Sugihara, H.; Dan-oh, Y.; Kasada, C.; Shinpo, A.; Suga, S. *J. Phys. Chem. B* **2005**, *109*, 15476−15482.
(38) Kim, S.; Lee, J. K.; Kang, S. O.; Ko, J.; Yum, J. H.; Fantacci, S.; Angelis, F. D.; Nazeeruddin, M. K.; Grätzel, M. *J. Am. Chem. Soc.* **2006**, *128*, 16701−16707.
(39) (a) Koumura, N.; Wang, Z. S.; Mori, S.; Miyashita, M.; Suzuki, E.; Hara, K. *J. Am. Chem. Soc.* **2006**, *128*, 14256−14257. (b) Wang, Z. S.; Koumura, N.; Cui, Y.; Takahashi, M.; Sekiguchi, H.; Mori, A.; Kubo, T.; Furube, A.; Hara, K. *Chem. Mater.* **2008**, *20*, 3993−4003.
(40) Wang, Z. S.; Cui, Y.; Hara, K.; Dan-oh, Y.; Kasada, C.; Shinpo, A. *Adv. Mater.* **2007**, *19*, 1138−1141.
(41) Hwang, S.; Lee, J. H.; Park, C.; Lee, H.; Kim, C.; Park, C.; Lee, M.-H.; Lee, W.; Park, J.; Kim, K.; Park, N.-G.; Kim, C. *Chem. Commun.* **2007**, *2007*, 4887−4889.
(42) Ito, S.; Miura, H.; Uchida, S.; Takata, M.; Sumioka, K.; Liska, P.; Comte, P.; Pechy, P.; Grätzel, M. *Chem. Commun.* **2008**, *2008*, 5194−5196.
(43) (a) O'Regan, B.; Grätzel, M. *Nature* **1991**, *353*, 737−739. (b) Nazeeruddin, M. K.; Kay, A.; Rodicio, I.; Humphry-Baker, R.; Müller, E.; Liska, P.; Vlachopoulos, N.; Grätzel, M. *J. Am. Chem. Soc.* **1993**, *115*, 6382−6390. (c) Hagfeldt, A.; Grätzel, M. *Chem. Rev.* **1995**, *95*, 49−68.
(44) (a) Hashimoto, K.; Kawai, T.; Sakata, T. *Nouv. J. Chim.* **1983**, *7*, 249−253. (b) Misawa, H.; Sakuragi, H.; Usui, Y.; Tokumaru, K. *Chem. Lett.* **1983**, 4516−4517. (c) Shimizu, T.; Iyoda, T.; Koide, Y. *J. Am. Chem. Soc.* **1985**, *107*, 35−41. (d) Malinka, E. A.; Kamalov, G. L.; Vodzinskii, S. V.; Melnik, V. I.; Zhilina, Z. I. *J. Photochem. Photobiol., A* **1995**, *90*, 153−158. (e) Abe, R.; Hara, K.; Sayama, K.; Domen, K.; Arakawa, H. *J. Photochem. Photobiol., A* **2000**, *137*, 63−69. (f) Tennakone, K.; Bandara, J. *Appl. Catal., A* **2001**, *208*, 335−341.
(45) Kim, Y. I.; Salim, S.; Huq, M. J.; Mallouk, T. E. *J. Am. Chem. Soc.* **1991**, *113*, 9561−9563.
(46) Kim, Y. I.; Atherton, S. J.; Brigham, E. S.; Mallouk, T. E. *J. Phys. Chem.* **1993**, *97*, 11802−11810.
(47) Saupe, G. B.; Mallouk, T. E.; Kim, W.; Schmehl, R. H. *J. Phys. Chem. B* **1997**, *101*, 2508−2513.
(48) Abe, R.; Sayama, K.; Arakawa, H. *Chem. Phys. Lett.* **2003**, *379*, 230−235.
(49) Abe, R.; Sayama, K.; Arakawa, H. *J. Photochem. Photobiol., A* **2004**, *166*, 115−122.
(50) Ikeda, S.; Tanaka, A.; Shinohara, K.; Hara, M.; Kondo, J. N.; Maruya, K.; Domen, K. *Microporous Mater.* **1997**, *9*, 253−258.
(51) Sayama, K.; Tanaka, A.; Domen, K.; Maruya, K.; Onishi, T. *J. Phys. Chem.* **1991**, *95*, 1345−1348.
(52) Heimer, T. A.; D'Arcangelis, S. T.; Farzad, F.; Stipkala, J. M.; Meyer, G. J. *Inorg. Chem.* **1996**, *35*, 5319−5324.
(53) Katoh, R.; Furube, A.; Mori, S.; Miyashita, M.; Sunahara, K.; Koumura, N.; Hara, K. *Energy Environ. Sci* **2009**, *2*, 542−546.
(54) (a) Harriman, A.; Pickering, I. J.; Thomas, J. M.; Christensen, P. A. *J. Chem. Soc., Faraday Trans. 1* **1988**, *84*, 2795−2806. (b) Hara, M.; Waraksa, C. C.; Lean, J. T.; Lewis, B. A.; Mallouk, T. E. *J. Phys. Chem. A* **2000**, *104*, 5275−5280.
(55) Daeneke, T.; Uemura, Y.; Duffy, N. W.; Mozer, A. J.; Koumura, N.; Bach, U.; Spiccia, L. *Adv. Mater.* **2012**, *24*, 1222−1225.